A kinase interacting protein (AKIP1) is a key regulator of cardiac stress

Mira Sastri[a,b,1], Kristofer J. Haushalter[a], Mathivadhani Panneerselvam[b], Philip Chang[a], Heidi Fridolfsson[b], J. Cameron Finley[b], Daniel Ng[b], Jan M. Schilling[b], Atsushi Miyanohara[c], Michele E. Day[d], Hiro Hakozaki[e], Susanna Petrosyan[f], Antonius Koller[g], Charles C. King[c], Manjula Darshi[h], Donald K. Blumenthal[i], Sameh Saad Ali[j], David M. Roth[b,j], Hemal H. Patel[b,i,1,2], and Susan S. Taylor[a,f,h,1,2]

Departments of [a]Biochemistry and Chemistry, [b]Anesthesiology, [c]Pediatrics, and [f]Pharmacology, [d]San Diego Supercomputer Center, and [e]National Center for Microscopy and Imaging Research, University of California at San Diego, La Jolla, CA 92093; [g]Proteomics Center, Stony Brook University Medical Center, Stony Brook, NY 11794-8691; [h]Howard Hughes Medical Institute, University of California at San Diego, La Jolla, CA 92093; [i]Department of Pharmacology and Toxicology, University of Utah College of Pharmacy, Salt Lake City, UT 84112; and [j]VA San Diego Healthcare System, San Diego, CA 92161

Contributed by Susan S. Taylor, December 14, 2012 (sent for review October 24, 2012)

cAMP-dependent protein kinase (PKA) regulates a myriad of functions in the heart, including cardiac contractility, myocardial metabolism, and gene expression. However, a molecular integrator of the PKA response in the heart is unknown. Here, we show that the PKA adaptor A-kinase interacting protein 1 (AKIP1) is up-regulated in cardiac myocytes in response to oxidant stress. Mice with cardiac gene transfer of AKIP1 have enhanced protection to ischemic stress. We hypothesized that this adaptation to stress was mitochondrial-dependent. AKIP1 interacted with the mitochondrial localized apoptosis inducing factor (AIF) under both normal and oxidant stress. When cardiac myocytes or whole hearts are exposed to oxidant and ischemic stress, levels of both AKIP1 and AIF were enhanced. AKIP1 is preferentially localized to interfibrillary mitochondria and up-regulated in this cardiac mitochondrial subpopulation on ischemic injury. Mitochondria isolated from AKIP1 gene-transferred hearts showed increased mitochondrial localization of AKIP1, decreased reactive oxygen species generation, enhanced calcium tolerance, decreased mitochondrial cytochrome C release, and enhance phosphorylation of mitochondrial PKA substrates on ischemic stress. These observations highlight AKIP1 as a critical molecular regulator and a therapeutic control point for stress adaptation in the heart.

ischemia/reperfusion | oxidative stress

Cardiovascular disease remains a major cause of morbidity and mortality in the United States. There is limited insight into the key molecular mechanisms that regulate the physiological and pathological signals in the heart. Ischemic stress causes damage to the heart, resulting in myocardial infarction, heart failure, and ischemic heart disease. One way that the heart adapts to ischemia/reperfusion (I/R) injury is through an innate protective mechanism termed ischemic preconditioning. This preconditioning occurs when the myocardium is exposed to brief ischemia, resulting in protection from subsequent prolonged ischemia (1). Autophagy, apoptosis, and necrosis are important cellular mechanisms that mediate this stress-induced damage control (2–5). Despite considerable data describing the signaling events leading to cardiac protection, clinical translation is limited for ischemic heart disease.

Cardiac myocytes are terminally differentiated, and processes that control cell death and survival in myocytes are tightly regulated. cAMP-dependent protein kinase (PKA) has distinct, albeit dichotomous, roles in the heart, wherein it can lead to either cell survival or death (6–8). It is an inactive tetrameric holoenzyme composed of two catalytic (PKAc) and two regulatory subunits that dissociate on cAMP binding, allowing PKAc to activate downstream signaling events. PKA has been linked to a number of cardiac pathologies, such as ischemic heart disease, dilated cardiomyopathy, and heart failure (9–11). However, the key molecular switch for regulating diverse PKA signaling is not known.

A kinase interacting protein (AKIP1/BCA3), a PKAc adaptor, was first discovered in mRNA screens of breast and prostate cancer cell lines (12). AKIP1 was found through a yeast two-hybrid screen as a protein of unknown function that interacted with the N-terminal 30 residues of PKAc (13). In humans, there are three splice variants, the full-length protein (AKIP1a), one that lacks the third exon (AKIP1b), and one that lacks the third and fifth exons (AKIP1c). In contrast, only the full-length protein is present in rodents (14). The literature is quite limited on both the biochemical and biological roles of AKIP1. AKIP1 has been shown to scaffold NF-κB in a PKA phosphorylation-dependent manner and regulate transcription. This regulation is dependent on the splice variants of AKIP1. AKIP1b was shown to recruit the histone deacetylase silent mating type information regulation 2 homolog (SIRT1) in a NEDDylation (NEDD8, neural precursor cell expressed, developmentally down-regulated 8-mediated)-dependent manner and repress transcription (15). In contrast, AKIP1a was shown to recruit NF-κB in a PKA-dependent manner and enhance transcription (16).

Although the AKIP1 gene was shown to be up-regulated in heart failure (17), its functional importance in the heart is unknown. Because AKIP1 interacts with PKAc, we hypothesized that AKIP1 is a putative molecular integrator regulating myocyte death and survival. In this paper, we describe AKIP1 as an early-

Significance

Early signaling events leading to protection in the heart under cardiac injury are poorly understood. We identified one such protein, A kinase interacting protein (AKIP1), as a modulator that responds to oxidative stress; up-regulation of AKIP1 showed protection to ischemic injury through enhanced mitochondrial integrity. We show AKIP1 functions as a molecular scaffold via interaction with mitochondrial apoptosis inducing factor and increases protein kinase A activity. These mitochondrial signaling complexes assembled by AKIP1 alter the physiological response of the heart under ischemic stress. Understanding molecular activity and regulation of AKIP1 could lead to novel therapeutic approaches to limit myocardial injury.

Author contributions: M.S. and H.H.P. designed research; M.S., K.J.H., M.P., P.C., H.F., J.C.F., D.N., J.M.S., and M.E.D. performed research; A.M., S.P., A.K., C.C.K., M.D., S.S.A., and H.H.P., contributed new reagents/analytic tools; M.S., K.J.H., H.F., J.C.F., D.K.B., D.M.R., H.H.P., and S.S.T. analyzed data; and M.S. wrote the paper.

The authors declare no conflict of interest.

Freely available online through the PNAS open access option.

[1]To whom correspondence may be addressed. E-mail: msastri@ucsd.edu, hepatel@ucsd.edu, or staylor@ucsd.edu.

[2]H.H.P. and S.S.T. contributed equally to this work.

This article contains supporting information online at www.pnas.org/lookup/suppl/doi:10.1073/pnas.1221670110/-/DCSupplemental.

response protein triggered by oxidative stress. We show that AKIP1 is induced by oxidant stress in cardiac myocytes. Gene therapy to increase cardiac AKIP1 led to increased PKA signaling, improved cardiac function, and enhanced mitochondrial protection on ischemic stress. We also show a stress response interaction of AKIP1 with the mitochondria protein apoptosis-inducing factor (AIF). Such data suggest the potential of AKIP1 as a therapeutic target to modulate mitochondrial function in adaptation to cardiac stress.

Results

AKIP1 Is Expressed in the Heart and Elevated on Oxidant Stress. Previous studies from our laboratory and other groups show that AKIP1 is present in a number of cell lines and tissues (12, 13). Although AKIP1 was initially found to be elevated in breast and prostate cancer cell lines, our studies show that there is an extremely low amount of this protein in cultured cells lines such as HeLa, MDA-MB231, and HEK 293 (Fig. 1 *A* and *B*). We had to resort to the use of femto-maximum sensitivity substrate to detect AKIP1 in these cell lines. Even then, we were able to detect only AKIP1b isoform (Fig. S1). The only cell line that had detectable levels of the protein was DU145; however, here, we see considerable degradation of endogenous AKIP1 (Fig. 1*B*). Because there is a significant amount of AKIP1 mRNA in mouse hearts, we then did Western blot analysis of isolated adult rat ventricular myocytes (ARVMs) and found the presence of intact AKIP1 (Fig. 1*C*). In cardiac tissues, oxidative stress plays a pivotal role in both in myocardial energetics and end-stage heart failure (18, 19). Treatment of neonatal rat ventricular myocytes (NRVMs) with hydrogen peroxide (H_2O_2) increased the level of AKIP1 within 15 min (Fig. 1*D*). Because this treatment was to mimic oxidant stress, we then determined the effect of hypoxia and hypoxia/reoxygenation (H/R; as additional models of simulated in vitro ischemic stress) on AKIP1 expression. When ARVMs were exposed to hypoxia with and without reoxygenation, AKIP1 expression was elevated within 15 min of hypoxia and sustained on oxidant stress for up to 60 min of reoxygenation. During reoxygenation, there was cellular activation of hypoxia-inducible factor 1, alpha subunit (basic helix-loop-helix transcription factor) (HIF1α) with no change in PKA (Fig. 1*E*). We had identified AKIP1 as a PKA binding protein important in the retention and activity of PKA signaling (13, 20), and PKA is thought to be essential in hypoxia and H/R (21). In ARVMs exposed to hypoxia and H/R, as expected, there was enhanced colocalization between AKIP1 and PKAc (Fig. 1*F*).

AKIP1 Overexpression Protects the Heart from I/R Injury. To further define the role of AKIP1 in the heart, we designed tetracycline (TET) -off adenoviral expression systems to overexpress AKIP1 (Ad-AKIP1). In ARVMs, there was robust expression of AKIP1 with the TET-off regulated adenovirus (Fig. 2*A*). To confirm that there was no change in localization on viral transduction, immunofluorescence of Ad-AKIP1 and Ad-Empty vector was carried out (Fig. 2*B*). The efficacy of these viruses at the organ level was tested by performing indirect intracoronary gene transfer of the TET-off AKIP1 adenovirus followed by 7 d of in vivo incubation, after which hearts were excised and recovery of cardiac function after I/R injury was assessed in Langendorff-perfused hearts. After 25 min of global no-flow ischemia and 45 min of reperfusion, developed pressure, end diastolic pressure, and $^{\pm}$dP/dt

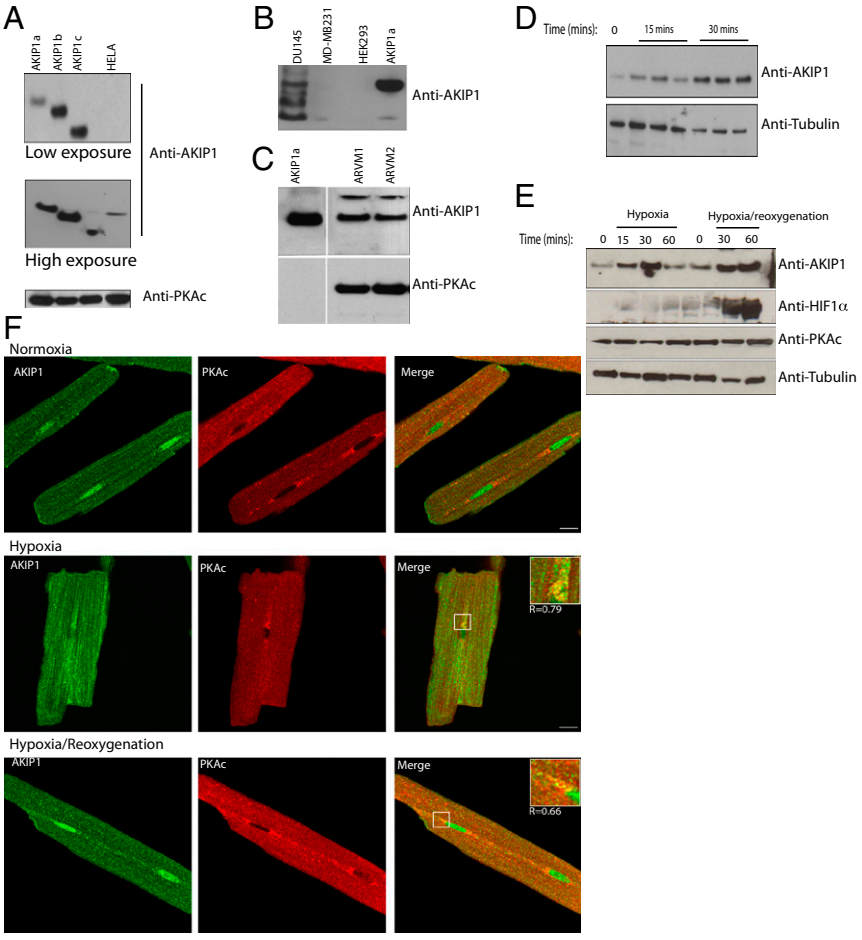

Fig. 1. Endogenous AKIP1 is present in cardiac myocytes and up-regulated in response to oxidant stress. (*A*) Endogenous AKIP1 showed very low expression in HeLa cells. Overexpressed AKIP1 splice variants were used as controls. (*B*) AKIP1 was present in prostate (DU145), and in breast (MDA-MB231) and HEK 293, the expression was minimal. (*C*) In contrast, ARVMs had a relatively higher level of endogenous AKIP1, and PKA was used as a loading control. (*D*) Neonatal rat cardiac myocytes exposed to hydrogen peroxide (100 μM) showed up-regulation of AKIP1 expression on stress. (*E*) ARVMs were subjected to hypoxia for the times indicated, and reoxygenation was performed after 30 min hypoxia. AKIP1 expression increased during both hypoxia and H/R; HIF1α levels increased during reoxygenation, whereas PKA levels remained unchanged. (*F*) Imaging of ARVMs exposed to 30-min hypoxia or 30-min hypoxia/2-h reoxygenation showed enhanced colocalization AKIP1 (green), PKAc (red), and merge (yellow) compared with no treatment as shown by Pearson's coefficient *R* values (*Insets*). (Scale bars: 10 μM.)

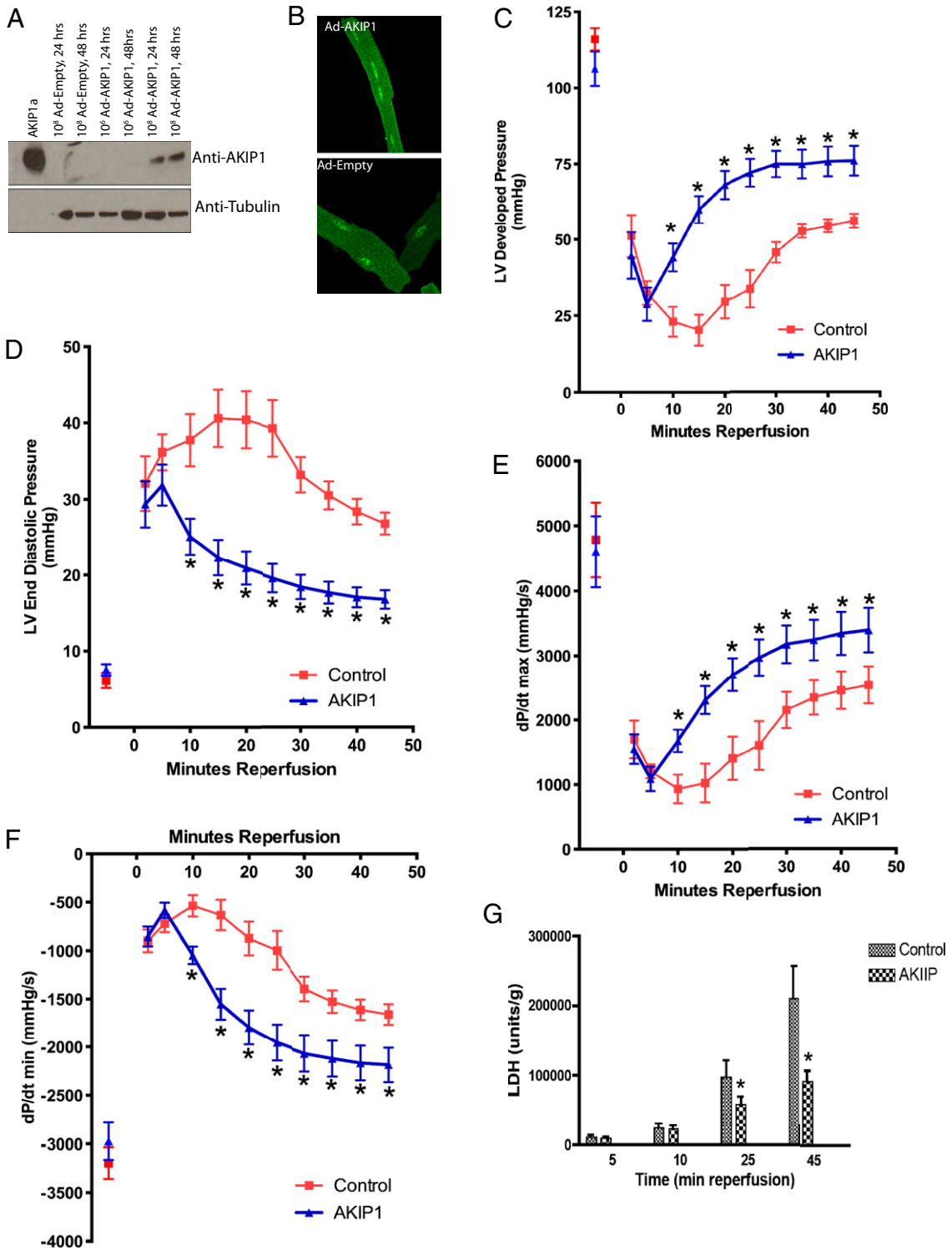

Fig. 2. AKIP1 overexpression protects from I/R injury. (*A*) AKIP1 vector was generated as an adenoviral TET-off system. ARVMs were treated with Ad-AKIP1 adenovirus for 24 and 48 h; some samples were treated with Ad-Empty, and others were treated with Ad-AKIP1 TET-off at the viral titer indicated. Ad-AKIP1 resulted in increased expression of AKIP1 at 48 h. (*B*) There was no change in localization because of either adenoviral expression or Ad-AKIP1 overexpression. (*C*–*G*) Mice were gene-transferred by indirect intracoronary injection with 1×10^9 viral particles of TET-off Ad-AKIP1 and allowed to recover for 7 d. On the seventh day, hearts were excised and perfused on a Langendorff apparatus to determine tolerance to I/R injury. Hearts were subjected to 25 min of global no-flow ischemia, and functional recovery was measured up to 45 min of reperfusion. Developed pressure (*C*), end diastolic pressure (*D*), and $^{\pm}$dP/dt (*E* and *F*) were improved with AKIP1 overexpression. This functional improvement was confirmed by measuring LDH levels in effluent at various times of reperfusion. (*G*) LDH release was significantly reduced with AKIP1 overexpression (*$P < 0.05$.); n = 8–9 per group for all studies.

parameters were measured. AKIP1 overexpression augmented recovery of cardiac function as shown by increased developed pressure (Fig. 2*C*), decreased diastolic dysfunction (Fig. 2*D*), increased inotropic state (force of muscle contraction) (Fig. 2*E*), and increased Lusitropic state (myocardial relaxation) (Fig. 2*F*). This protective effect at the functional level was further confirmed by measuring lactate dehydrogenase (LDH; an enzyme that is released from necrotic cardiac myocytes) release in the effluent, where AKIP1 overexpressing hearts had a significantly reduced LDH level throughout 45 min of reperfusion (Fig. 2*G*).

AKIP1 Is Localized at the Mitochondria and Interacts with AIF. Protection from ischemic injury in the heart has been directly linked to altered mitochondrial function (22, 23). Therefore, we determined whether endogenous AKIP1 was localized to the mitochondria in resting hearts. Previously, we had reported AKIP1 as a nuclear protein (13). Mitochondrial and nuclear fractions were isolated from WT rat hearts, and AKIP1 was present in both the organelles (Fig. 3*A*). Nuclear contamination of the mitochondria was assessed using p84. Because mitochondria are associated with endoplasmic reticulum (ER) (24), additional rounds of purification were performed to reduce ER contamination (indicated by the reduced levels of Calreticulin). There was enrichment of AKIP1 at the mitochondria (Fig. 3*B*). To validate these findings, ARVMs were stained for AKIP1, cytochrome C (mitochondrial marker), and poly(ADP-ribose) polymerase 1 (PARP1) (nuclear marker). At the basal level, AKIP1 was present at both the mitochondria and the nucleus (Fig. 3*C*). Protein–protein interactions are one of the mechanisms to glean insight into the function. MS was, therefore, used to determine AKIP1-interacting proteins. GST isoforms of AKIP1 were used in pull-down experiments, and the bands that were unique among each other and from the GST controls as indicated by the arrow (Fig. 3*D*) were analyzed using nanoliquid chromatography tandem MS. The peptides were identified as Programmed Cell death protein 8/AIF (Table 1) and heat shock protein 70 (Hsp-70) (Table S1). These interactions were confirmed by Western blot analysis (Fig. 3*E*). AIF is a dual specific protein that functions at the mitochondria as an FAD-dependent NADH oxidase, and on apoptosis, it translocates to the nucleus to bring about cell death (25). AIF interacted mainly with AKIP1a (the isoform present in both humans and rodents), whereas Hsp-70 interacted with all three AKIP1 isoforms. Because there is only 70% homology between the mouse and human AKIP1a, we also verified the interaction with AIF using GST mouse AKIP1 (Fig. S2). We failed to show the interaction of the endogenous AKIP1 with AIF by coimmunoprecipitation, because endogenous AKIP1 was highly susceptible to proteolytic degradation, even in the presence of protease inhibitors.

Oxidant and Hypoxic Stress Did Not Affect Binding of AIF to AKIP1 in Vitro. Reactive oxygen species (ROS) are known to be mediators of intracellular signaling pathways through protein–protein interactions. Because AKIP1 was protective to the heart, we addressed the question of whether AKIP1 could interact with AIF on oxidant

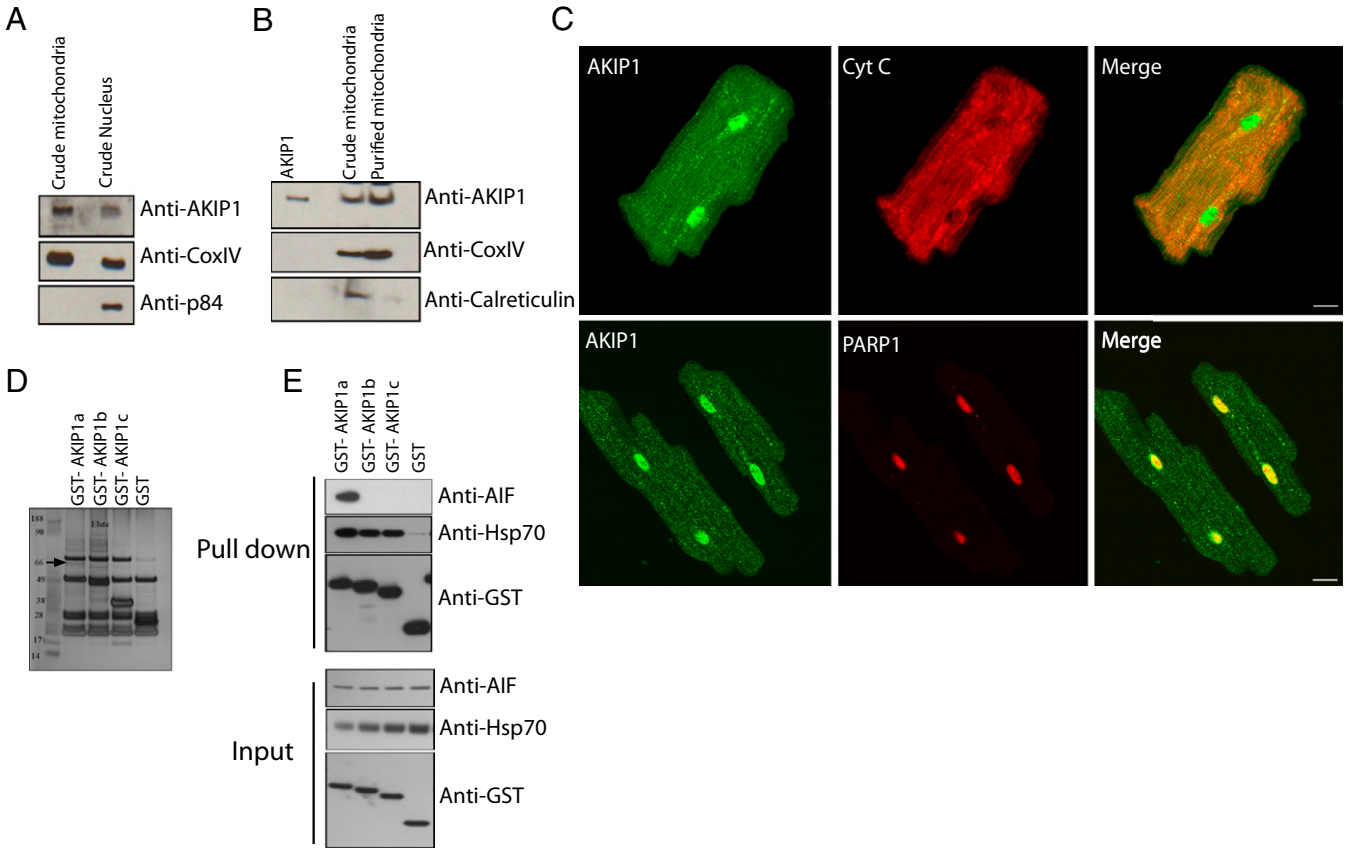

Fig. 3. AKIP1 localizes to the mitochondria and interacts with AIF. (*A*) Rat heart fractionation showed that AKIP1 was present in both the mitochondria and the nuclear fractions. CoxIV and p84 were used as mitochondrial and nuclear markers, respectively. (*B*) Percoll-purified mitochondria showed enrichment of AKIP1. ER contamination was assessed by calreticulin. (*C*) Adult cardiac myocytes were costained with AKIP1 (green) and cytochrome C (a mitochondrial marker; red) as well as PARP1 (a nuclear marker; red). AKIP1 showed basal localization with both mitochondria and nuclei. (*D*) GST constructs of AKIP1 splice variants were used to pull down endogenous proteins in HEK293 cells and analyzed by Coomassie staining to determine novel interacting proteins. The unique band in GST-AKIP1a indicated by an arrow was determined to be AIF and Hsp-70. (*E*) GST-AKIP1a interacted with AIF, and all of the isoforms interacted with Hsp-70.

Table 1. List of peptides from AIF identified by MS

Rank	Log (e)	Log (I)	Percent	No.	Total	M_r	Accession
1	−40.9	3.46	22	5	15	23.3	gi[230338] gpmDB homolog protein Chain E, Trypsin (E.C. 3.4.21.4) Complex with Bowman–Birk Inhibitor
2	−17.9	2.22	5.1	3	3	66.0	ENSP00000252244 gpmDB homolog protein Keratin, type II cytoskeletal1
3	−8.7	2.06	8.4	1	1	24.5	gi[115646] gpmDB homolog protein α-s1 casein precursor
4	−5.5	1.52	3.1	1	1	58.8	ENSP00000269576 gpmDB homolog protein Keratin, type 1 cytoskeletal
5	−4.2	1.74	4.0	1	1	35.6	ENSP00000316320 gpmDB homolog protein Programmed cell death protein 8, mitochondrial precursor (AIF)
6	−1.3	1.72	3.7	1	1	25.9	ENSP0000034280 gpmDB homolog protein Trypsin 1 precursor
7	−1.2	2.03	7.1	1	1	34.5	ENSP00000216891 gpmDB homolog protein Mitochondrial import receptor subunit TOM34 (translocase of outer membrane 34-kDa subunit; hTOM34)

List of peptides from AIF identified by MS. The band from GST-AKIP1 pull down was excised from the gel and in situ-digested, and the peptides were extracted. The resulting peptides were analyzed by nanoliquid chromatography tandem MS. Log (e), log (expectation value for the peptide match); Δm, difference (error) between the experimental and calculated masses; sequence, identified peptide sequence; *z*, charge state.

stress. HEK 293 cells were transfected with GST-AKIP1 and streptavidin binding protein-tagged AIF and treated with H_20_2 for the times indicated followed by streptavidin pull down. The results showed that AKIP1 interacted with AIF for up to 30 min of treatment (Fig. 4*A*). In cardiac cells, under high oxidant stress, AIF has been shown to translocate from the mitochondria to the nucleus to induce cell death in a caspase-independent manner (26). However, little is known about AIF under mild and short duration of ROS generation. Because AKIP1 levels increase under these conditions, the effect on the colocalization with AIF was monitored by indirect immunofluorescence. Under basal conditions, there was weak fluorescence staining and little colocalization between AKIP1 and AIF. However, there was increased colocalization in ARVMs within 15 min of H_2O_2 treatment that was sustained for up to 45 min of treatment (Fig. 4*B*). To dissect the effects of oxidant stress on AIF, hypoxia and H/R were induced in the isolated ARVM cells. There was enhanced AIF expression on oxidant stress that correlated with the increased AKIP1 expression (Fig. 4*C*). This observation was confirmed by immunofluorescence, wherein there was enhanced colocalization between AKIP1 and AIF on hypoxia as well as H/R (Fig. 4*D*).

In Vivo I/R Stress-Induced AKIP1 Expression in Interfibrillary Mitochondria. To further validate AKIP1 induction in vivo, mice were subjected to 30 min ischemia followed by 2 h reperfusion. This in vivo I/R stress caused increased levels of both AKIP1 and AIF with no change in PKA (Fig. 5*A*). Because AKIP1 was present both at the nucleus and the mitochondria and induced on stress, we wanted to establish whether the increase was because of changes in localization. Hearts from control and I/R-exposed mice were fractionated into cytosol, membrane/mitochondria, nuclear, and nuclear/cytoskeleton fractions, with purity determined by appropriate markers. Under ischemic stress, there was an increase in the level of AKIP1 in both the membrane and the nuclear/cytoskeletal fractions, although there seemed to be no change in localization (Fig. 5*B*). In the heart, there are two distinct subpopulations of mitochondria, interfibrillary (IFM) and subsarcrolemmal (SSM), and studies show that IFM and SSM have differential response to metabolic stress (27, 28). These two subpopulations were isolated from WT hearts, and mitochondrial function and AKIP localization were assessed. IFM showed increased state 4 [without ADP and with malate/pyruvate (complex 1)], state 3 [with ADP and with succinate (complex II)], and complex IV respiration relative to SSM (Fig. 5*C*). AKIP1 was present in both the fractions, although it was more abundant in the IFM as normalized against a mitochondrial matrix protein, GRP-75 (Fig. 5*D*). We went onto determine if, under stress, when AKIP1 is up-regulated, it preferentially compartments into a specific mitochondrial subpopulation. IFM isolated from hearts that underwent I/R (25-min ischemia and 10-min reperfusion) had increased expression of AKIP1 (Fig. 5*E*), whereas SSM showed no change (data not shown). Ischemic stress results in both hypoxia and substrate/glucose deprivation, which causes oxidative stress (29). To recapitulate these conditions in vitro, ARVMs were exposed to hypoxia in a glucose-free medium followed by reoxygenation (H/R). Both AKIP1 and AIF colocalized on H/R in ARVMs (Fig. 5*F*). This colocalization was more intense in IFM, which was shown by the merge with the IFM marker mitofilin (30) (Fig. 5*G*), confirming our fractionation and immunoblot data.

AKIP1 Overexpression Increases Mitochondrial-Localized AKIP1, Adapts Mitochondria to Stress, and Enhances Mitochondrial PKA Activity. Because mitochondria are the end effectors of protection, we carefully determined the impact of AKIP1 on mitochondrial integrity. Mouse hearts gene-transferred with the Ad-AKIP1 and Ad-Empty were subjected ex vivo to 25-min ischemia followed by 5-min reperfusion, after which crude mitochondrial fractions were prepared for functional analysis. There was increased expression of AKIP1 in mitochondria after gene transfer (Fig. 6*A*). A key feature of mitochondria in the setting of I/R injury is generation of ROS (31, 32) leading to reperfusion injury. Electron paramagnetic resonance (EPR) showed decreased ROS generation in mitochondria, indicating more tightly coupled respiration from AKIP1-overexpressing hearts under both states 3 and 4 respiration with complex I substrates (Fig. 6*B*). Mitochondrial swelling, indicative of mitochondrial permeability transition pore opening, was decreased in AKIP1 gene-transferred hearts (Fig. 6*C*) as was the release of cytochrome C from mitochondria to the cytosolic fraction (Fig. 6*D*). PKA signaling has been shown to affect mitochondrial redox state through ROS production (33). Because PKAc and AKIP1 interact, this protein complex may also influence PKAc substrates, possibly in the mitochondria. Therefore, mitochondrial fractions from AKIP1 gene-transferred hearts showed two distinct phosphorylated proteins of 20 and 60 kDa (Fig. 6*E*). MS identified the 60-kDa protein as ATP synthase α-subunit, whereas the 20-kDa band could not be identified because of the low abundance. Scansite (http://scansite3.mit.edu) analysis of ATP synthase α-subunit sequence identified a putative PKA phosphorylation site (Fig. S3). Identification of the site(s) of phosphorylation and significance is currently under investigation. Ischemic stress not only increased AKIP1 levels in vivo, but also, there was increased expression of ATP synthase-α (Fig. 6*F*). As anticipated, PKAc levels did not change, and Hsp-90 was used as a loading control. This increase was confirmed by colocalization of PKA and ATP synthase-α with AKIP1 under stimulated ischemia (Fig. 6 *G* and *H*). Collectively, these data suggest that AKIP1 could modulate mitochondrial dynamics and function under oxidant stress, leading to protection.

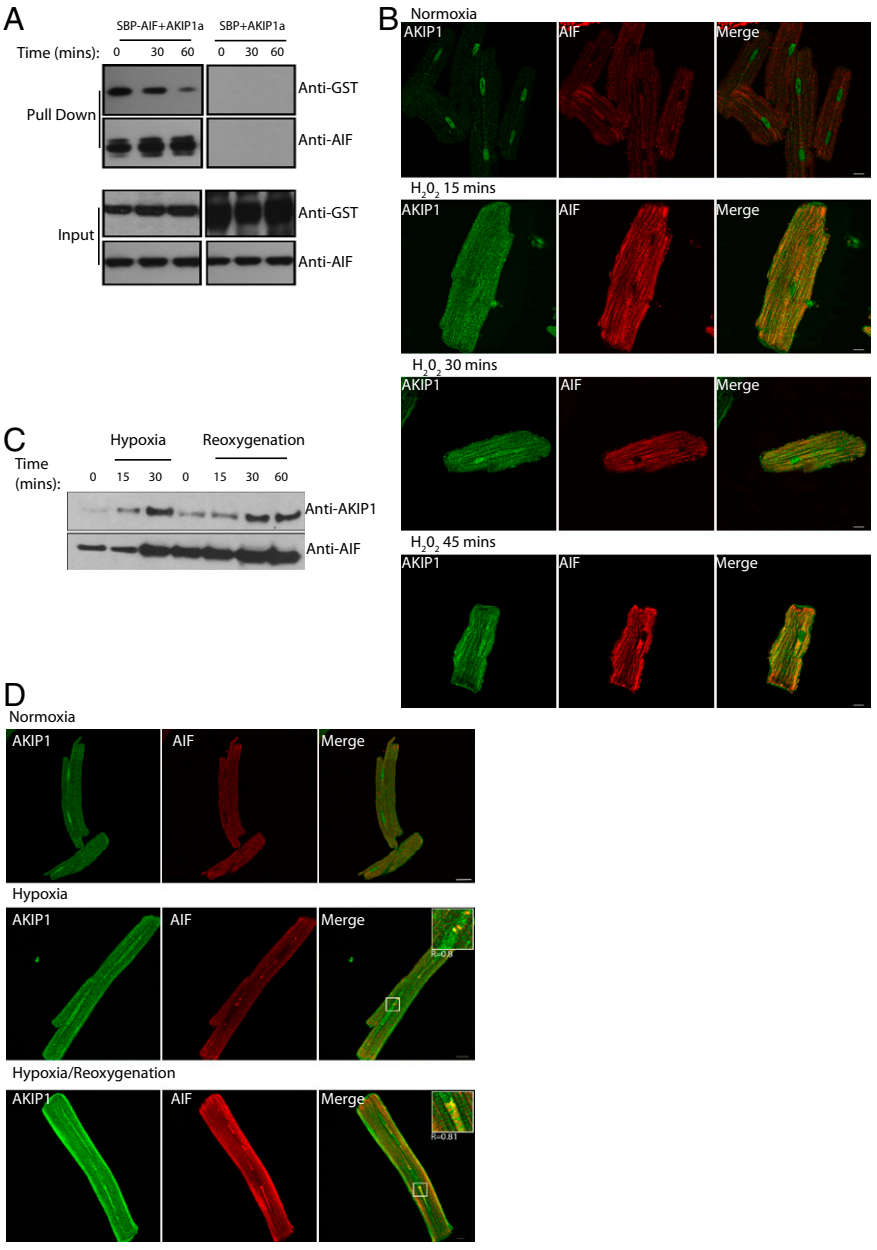

Fig. 4. In vitro interaction of AKIP1 and AIF is unchanged on mild oxidative stress. (*A*) Streptavidin binding protein-tagged AIF and GST-AKIP1 splice variants were transfected into HEK293 cells, and the cells were treated with H_2O_2 for the times indicated. Streptavidin beads were used to pull down the complexes. AKIP1a showed maximal binding up to 30 min of H_2O_2 treatment. (*B*) In ARVMs, there was enhanced expression and colocalization of AKIP1 (green) with AIF (red) on both H_2O_2 treatments. (*C* and *D*) This increase of AIF was seen both in hypoxia and H/R, (*C*) with enhanced colocalization with AKIP1 as magnified in *Insets* (*D*).

Discussion

Preconditioning is one of the most effective interventions to protect the heart from myocardial infarction (1, 34). However, clinical translation of this phenomenon has been limited. There are few reports about the induction of early-response genes during ischemic injury and reperfusion-induced oxidant stress (35–37). This study shows up-regulation of one such protein, AKIP1. We show increased levels of AKIP1 both in vitro and in vivo under short durations of ischemia and reperfusion (Figs. 1 and 5). We also show that overexpression of this protein was protective to the heart against I/R injury (Fig. 2). Exercise has been shown to mimic ischemic preconditioning and also lead to cardiac protection (38). Gene expression profiles of rat left ventricles after mild exercise showed elevated mRNA levels of cAMP response element binding protein (plausibly PKA-regulated), AKIP1, and HIF1α (39). Such findings are consistent with our observations and suggest that overexpression of AKIP1 may be a therapeutic approach for limiting cardiac injury.

There was an increased level of HIF1α with 30-min hypoxia followed by 2-h reperfusion concomitant with increased AKIP1 levels (Fig. 1). How does this early induction occur? Previously, we had shown, in most cell lines, that there is mRNA expression of AKIP1 (13). However, we were never able to detect protein expression, and this problem could be addressed through several mechanisms. One explanation could be that AKIP1 is rapidly regulated by microRNAs (Fig. S4) or through proteolytic degradation by specific interaction of AKIP1 with AIF or phosphorylation by PKA. These specific pathways will be discussed in future studies.

Gao et al. (40) in 2010 proposed that the levels of AKIP1 determined the cell fate. There are very few reports that comment on the function of AKIP1/BCA3. We believe that this protein has two distinct and crucial roles. The first role, as was previously published (16, 20), is at the nucleus, where it interacts and enhances the role of PKA/NF-κB/SIRT1, and the second role is at the mitochondria. A key feature of cardiac protection is regulation of mitochondria under ischemic stress (41, 42). Mitochondria

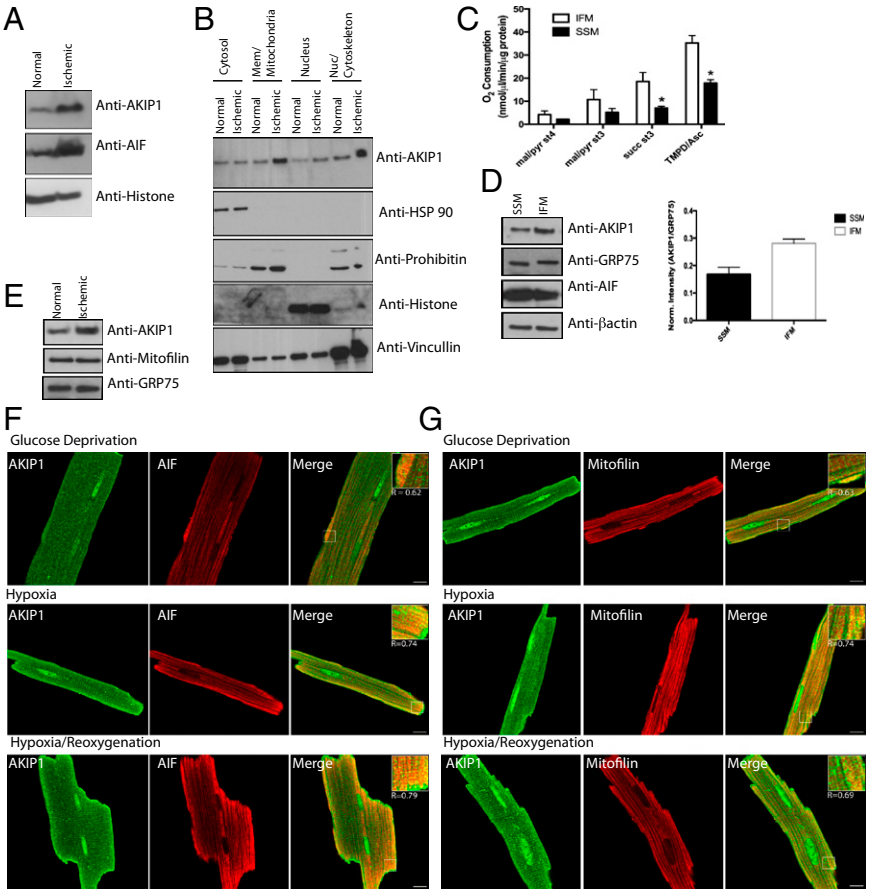

Fig. 5. I/R injury increases AKIP1 levels in interfibrillary mitochondria. (*A*) Hearts from control mice or mice subjected to 30-min ischemia/2-h reperfusion in vivo were analyzed for AKIP1 expression. AKIP1expression was increased with ischemic stress. Histone was used as a loading control. (*B*) Normal and ischemic mouse hearts were subfractionated, and AKIP1 showed enrichment in the membrane and nuclear fraction on ischemic stress. (*C*) Mitochondria were fractionated into SSM and IFM mitochondria, and their mitochondrial function was assessed in at least four independent experiments. As reported, IFM showed higher mitochondrial respiratory function under states 4 and 3 respiration, and complex IV activity was enhanced. Standard error of mean is indicated by an asterisk. (*D*) AKIP1 expression was present in both the subfractions with slightly higher levels in IFM as normalized against the mitochondrial matrix protein GRP-75. AIF was present in both the fractions (*E*). (*F* and *G*) AKIP1 colocalized with both AIF (*F*) and mitofilin (*G*; marker for IFM). (Scale bars: 10 μM.)

are a major source of energy in the heart, but cardiac myocyte survival is also dependent on mitochondrial function and dynamics, particularly during an ischemic event. Our data suggest that it is not just the level of AKIP1 per se that was important for cell survival but also, its mitochondrial localization. In the heart, we show the presence of endogenous AKIP1 at the mitochondria (Fig. 3), and this localization is impacted by stress. A single report shows that the overexpression of both AKIP1 and p73 resulted in an association at the mitochondria, leading to cell death (43). Our data show an enhanced survival potential for AKIP1 in mitochondria; however, there could be several factors that influence the downstream effects of AKIP1 on cell death and survival, including (but not limited to) isoform specificity, interaction with other proteins, transformed cell types used, and the extent of stress applied to the system. We found that overexpression of AKIP1 isoforms, like the endogenous protein, showed both nuclear and membrane/mitochondrial localization (Fig. S5), suggesting that there may be a nuclear–mitochondrial cross-talk leading to protection in certain systems.

AKIP1 is not only localized to the mitochondria, but through MS, we found that it interacts with AIF (Fig. 3). AIF is a multifunctional protein that has diverse functions in both the mitochondria and the nucleus. In the mitochondria, AIF is thought to stabilize complex I and required for cell survival, proliferation, and mitochondrial integrity (44). AIF was discovered as a caspase-independent death effector that is released from the mitochondria and translocates to the nucleus to cause chromatin condensation and DNA fragmentation (45). However, the specific pathway that causes the release of AIF from the mitochondria is not well-known, and in the heart, it may depend on the nature of the ischemic insult (46, 47). Because AKIP1 interacts with AIF, it may be important in sequestering AIF to the mitochondria and preventing cell death under low genotoxic stress by modulating mitochondrial membrane integrity. To support this hypothesis, our studies show decreased calcium swelling and cytochrome C release in mitochondria overexpressing AKIP1 (Fig. 6).

Damage to the mitochondria generates increased amounts of ROS and produces less ATP-triggering apoptosis (18). Aberrant PKA signaling has been implicated in the production of oxidant stress, and previous studies from others and our laboratory have shown that PKA substrates, such as Drp-1 and ChChD3, were important in the maintenance of mitochondrial integrity (48, 49). Mitochondria isolated from Ad-AKIP1 gene-transferred hearts showed less ROS production (Fig. 6). Through changes in PKA signaling, we identified ATP synthase-α as a potential PKA phosphorylation target up-regulated in mitochondria from AKIP1 gene-transferred hearts (Fig. 6). Although ATP synthase-α has not been shown to be a substrate of PKA, it has been shown to bind to the 3′ UTR of dual specific A kinase anchoring protein-1 and regulate it (50). Furthermore, we show that ischemic stress that led to increased endogenous expression of AKIP1 also led to increased ATP synthase-α (Fig. 6). We postulate that, under physiological conditions, AKIP1 interaction with AIF and PKA could enhance the phosphorylation of ATP synthase-α. This phosphorylation could preclude the loss of membrane potential that is known to increase ROS production (51), thereby preventing the rupture of the mitochondrial membrane. In support of this hypothesis, a report has shown that down-regulation of ATP synthase-α caused the translocation of AIF into the nucleus on oxidant stress (28).

Mitochondrial subpopulation differences in the heart play an essential role in cardiovascular biology. Our data indicate that, although AKIP1 is associated with both SSM and IFM, it is more abundant in the IFM (Fig. 5). Previous studies have shown that, in aged mice, the levels of IFM go down because of ROS-induced

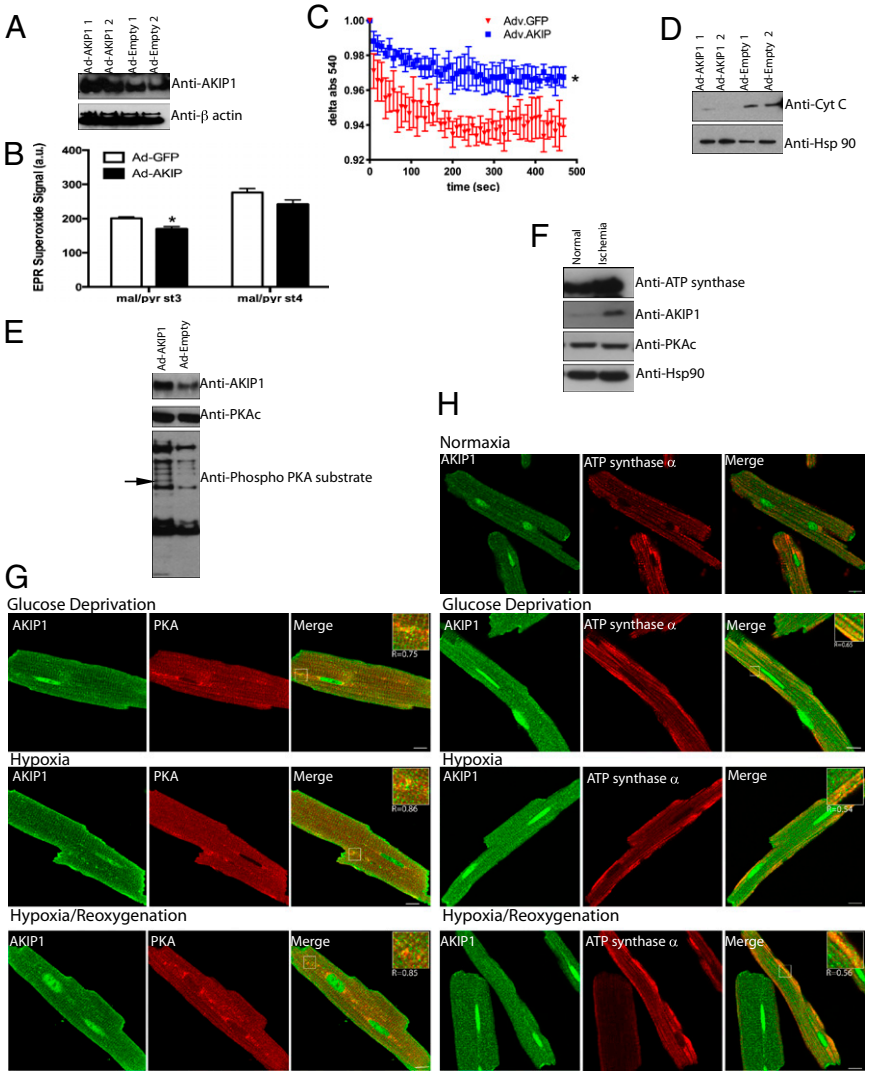

Fig. 6. Mice with cardiac AKIP1 gene transfer show increased mitochondrial protection and enhanced PKA signaling. (*A*) Mitochondria isolated from Ad-AKIP1 gene-transferred hearts show increased AKIP1 expression. (*B*) There was reduced stress-induced generation of ROS in mitochondria under states 4 and 3. (*C*) Ad-AKIP1 gene-transferred heart mitochondria were more resistant to calcium swelling compared with Ad-Empty. Standard error of mean is indicated by an asterisk. (*D*) During the course of mitochondrial purification, the cytosolic fractions were collected from both Ad-AKIP1 and Ad-Empty. Ad-AKIP1 samples showed decreased cytochrome C release. Hsp-90 was used as a loading control. (*E*) Ad-AKIP1 overexpression by gene transfer also showed enhanced PKA phosphorylation. The band indicated by the arrow was identified to be ATP synthase-α. (*F*) ATP synthase-α increased on I/R injury with no changes in PKA. Hsp-90 was used as a control. (*G* and *H*) Colocalization of AKIP1 with PKA and ATP synthase-α in ARVMs under stimulated ischemia. (Scale bars: 10 μM.)

damage to the mitochondria (27). Aged hearts are also more sensitive to ischemic stress (52). We predict that AKIP1 targeted to the mitochondria could be protective during aging and other cardiovascular diseases that lead to compromised mitochondrial function, because it would localize to and preserve function of IFM.

In conclusion, this study provides evidence for cardiac protection on acute stress through the induction of AKIP1. Our data identify AKIP1 as an essential and key molecular regulator/scaffold of heart function with several important translational implications. First, it provides us with a unique molecular target for acute cardiovascular stress. Second, because this protein has been implicated in breast and prostate cancer, it might have more general epidemiological implications in other systems and diseases. Third, the localization of and functional changes afforded to mitochondria by AKIP1 may serve as means to regulate energy and metabolism in a variety of disease settings.

Materials and Methods

Animal Care. Animals were treated according to the Guide for the Care and Use of Laboratory Animals (25). Animal protocols were approved by the Department of Veterans Affairs, San Diego Healthcare System, Institutional Animal Care and Use Committee. C57BL/6 male mice (8–10 wk and 24–26 g weight) were purchased from Jackson Laboratory and kept on a 12-h light/dark cycle in a temperature-controlled facility until the day of the experiment and had ad libitum access to food and water.

Langendorff-Perfused Hearts. Eight-week-old male mice (n = 8–9 for each group) were subjected to indirect intracoronary gene transfer (53) of the Ad-AKIP1 and Ad-GFP (1×10^9 viral particles), and the animals were allowed to recover for 7 d. After 7 d, hearts were excised and perfused on a Langendorff apparatus as previously described (54). After 15-min stabilization, hearts underwent 25 min of global, no-flow ischemia followed by 45 min of reperfusion. Cardiac parameters (developed pressure, $^{\pm}$dP/dt, end diastolic pressure, etc.) were continuously monitored. Additionally, perfusates were collected throughout for the measurement of LDH.

In Vivo I/R. Animals were randomly assigned to two groups as follows: sham and those mice that underwent in vivo I/R injury. Surgery was performed as previously described (55). Mice were anesthetized with pentobarbital sodium (80 mg/kg) and mechanically ventilated. Ischemia was produced by occluding the left coronary artery with a 7–0 silk suture on a tapered BV-1 needle (Ethicon) for 30 min. A small piece of polyethylene tubing was used to secure the silk ligature without damaging the artery. After 30 min of occlusion, the ligature was released, and the heart was reperfused for 2 h. Reperfusion was confirmed by observing return of blood flow in the epicardial coronary arteries.

Preparation of ARVMs and Addition of the Adenoviral Vectors. ARVMs were isolated from adult Sprague–Dawley rats (250–300 g, male) as described in detail previously (56). Myocytes were plated in heart media plus 4% FBS on laminin (2 μg/cm^2) -coated plates for 1 h. Plating media was changed to heart media supplemented with 1% BSA to remove all nonmyocytes, and ARVMs were placed in an incubator set at 37 °C and 5% CO_2 and incubated for 1–24 h before experiments. For the AKIP1 overexpression experiments,

after 2 h, adenovirus (Ad-AKIP1a and Ad-GFP) was added at 10^8 viral particles/mL, and the cells were allowed to recover for an additional 24 h. The cells were then collected in 10 mM Hepes, 60 mM KCl, 1 mM EDTA, and 0.5% Nonidet P-40 and sonicated using Misonix ultrasonic prossess (Qsonica). Protein concentrations were determined to get equal loads. Antitubulin, anti–β-actin, and Hsp-90 were used as loading controls. The NRVMs used in this study were a gift from Joan Heller Brown's laboratory (University of California at San Diego, La Jolla, CA).

Oxidative Stress Induction on Rat Adult Cardiomyocytes. Briefly, the isolated ARVMs were plated on 3-cm tissue culture dishes for Western blot analysis or glass coverslips (Fisher Scientific) precoated with laminin for imaging. These dishes and coverslips were placed in the CO_2 incubator for 24 h. Hypoxia was induced in isobaric Plexiglas chambers, where cells were exposed to 15 and 30 min 95%N_2/5%CO_2 gas flow. To induce oxidative stress after hypoxia, cells were returned to original conditions for an additional 1–2 h. Control cells were maintained under normoxic atmosphere. The cells on the 3-cm dishes were collected in 10 mM Hepes, 60 mM KCl, 1 mM EDTA, and 0.5% Nonidet P-40 and analyzed by Western blot. For the NRVM experiments, the cells were obtained in 6-cm cell culture plates, and they were treated with 100 μM H_2O_2 for the various times indicated. The cells were harvested and processed as indicated for ARVMs. The laminin-coated coverslips were either treated with 100 μM H_2O_2 or processed in hypoxic and H/R in a manner similar to the 6-cm dishes.

Mass Spectrometric Analysis. Bands were excised from SDS/PAGE gels and washed three times in 50% acetonitrile/10 mM NH_4HCO_3 followed by a brief dehydration in 100% acetonitrile. Proteins were incubated overnight in 50% acetonitrile/10 mM NH_4HCO_3 with 0.05 μg trypsin (Roche). Isolated peptides were washed and concentrated in C_{18} ZipTips (Millipore) according to the manufacturer's protocol. Samples were directly eluted onto a 100-spot platform using a buffer containing 4-α hydroxy cinnamic acid (Agilent), 50% acetonitrile, 10 mM diammonium citrate, and 0.1% trifluoroacetic acid. MALDI-TOF and subsequent MS/MS analysis of specific peptides were performed on an Applied Biosystems Q-Star XL hybrid mass spectrometer. MALDI-TOF fingerprint data were analyzed with the online database at Rockefeller University (http://prowl.rockefeller.edu), and MS/MS data were analyzed with the Mascot online database (http://www.matrixscience.com).

Immunofluorescence. The cells after the appropriate experiments were fixed with 4% paraformaldehyde (Electron Microscopy Sciences) for 15 min at room temperature. All solutions used during the immunostaining were prepared in 1× Dulbecco's PBS (Mediatech), and the immunostaining was performed and imaged as described previously. The following antibodies were used at 1:100 dilutions: anti-AIF (Cell Signaling), anti-AKIP1, which was raised in the rabbit in-house by Bethyl, Cy5-labeled donkey anti-rabbit IgG antibodies (Jackson ImmunoResearch Laboratories), and DyLight 649 (Jackson ImmunoResearch Laboratories). The cells were viewed with an Olympus FluoView1000 confocal laser scanning microscope equipped with an Olympus oil immersion 60× objective, N.A. 1.42. The collected confocal images were processed with Image J (57) to generate maximum intensity projection images (z = 30–40 slices; z step = 0.3 μm) and Adobe Photoshop to generate composite pictures. Colocalization analysis was performed using Co-Loc2 of the Fiji plug-in (58). To reduce the effects of background, noise, and cross-talk, only images that had Mander's coefficients, M1 and M2 > 0.5, were considered (59).

Isolation of Mouse Heart Mitochondria. Mice (n = 4) were killed, and hearts were removed. Ventricles were placed in ice-cold mitochondrial isolation medium (MIM; 0.3 M sucrose, 10 mM Hepes, 250 μM EDTA), minced, and homogenized with a Tissuemiser (Fisher Scientific). Homogenates were rinsed in MIM. Samples were centrifuged at 600 × g to clear nuclear/membrane debris. The resulting supernatant was spun at 8,000 × g for 15 min. The resulting pellet was resuspended in MIM in the presence of 1 mM BSA followed by another 8,000 × g spin for 15 min. The resulting pellet was resuspended in isolation buffer with BSA and spun again at 8,000 × g. To isolate pure mitochondria, the washing steps were repeated with MIM in a final 2-mL resuspension of the pellet in mitochondrial resuspension buffer (MRB; 500 mM EDTA, 250 mM mannitol, 5 mM Hepes). The mitochondria were layered on top of a 30% Percoll/70% MRB solution. The Percoll gradient was spun at 95,000 × g for 30 min. The mitochondrial band was removed from the gradient, and volume was increased 10-fold with MRB to remove the Percoll by centrifugation at 8,000 × g for 15 min. The mitochondrial pellet was resuspended in MRB and subjected to additional analysis.

Calcium Swelling. Calcium swelling was measured on an Infinite M200 plate reader at 540 nm over a span of 20 min. Crude mitochondria (0.5 μg/μL) in the absence of calcium were loaded onto a clear, flat-bottom 96-well plate and challenged with 250 mM calcium, with OD measured every 10 s. Change at 540 nm was compared between samples.

EPR Superoxide Measurement. For EPR studies, immediately after mixing mitochondria (0.1–0.2 mg protein) with 70 mM 5-(diisopropoxyphosphoryl)-5-ethyl-1-pyrroline-*N*-oxide and appropriate combinations of the substrates, the mixture was loaded into 500 glass capillary tubes and introduced into the EPR cavity of a MiniScope MS300 benchtop spectrometer (Magnettech GmbH). We confirmed that the detected EPR signals are substrate-specific and not caused by redox cycling in the studied mixtures by lack of signals when 5-(diisopropoxyphosphoryl)-5-ethyl-1-pyrroline-*N*-oxide was mixed with combinations of substrates and inhibitors in the absence of mitochondria. Assignment of the observed signals from mitochondria was confirmed through computer-assisted spectral simulation using the WinSim software. Signals were quantified by measuring the peak amplitudes of the observed spectra and normalized by mitochondrial protein concentrations.

Isolation of SSM and IFM from Mouse Heart. Methodology for mitochondrial subpopulation fractionation was adapted from Palmer et al. (60). Briefly, heart ventricular tissue from WT C57BL/6 mice (n = 4 for each group) was excised and homogenized in Chappell–Perry (CP) buffer (100 mM KCl, 50 mM Mops, pH 7.4, 5 mM $MgSO_4$*$7H_2O$, 1 mM EGTA, 1 mM ATP) supplemented with Protease Inhibitor (Roche). Homogenates was centrifuged at 500 × g for 10 min, and the resultant supernatant was further centrifuged at 8,000 × g for 10 min to yield the crude SSM pellet. For IFM, the pellet was resuspended in CP buffer supplemented with bovine trypsin (final concentration of 0.75 mg/mL) and then allowed to digest on ice for 15 min with frequent agitation. Digests were quenched CP buffer containing 0.2% BSA. Crude IFM pellets were isolated by a 500 × g spin to eliminate nuclear/myofibril contaminants followed by an 8,000 × g spin of the resulting supernatant. Crude SSM and IFM pellets were each suspended in 2 mL CP1 buffer without $MgSO_4$*$7H_2O$ and ATP and centrifuged again at 8,000 × g to yield isolated SSM and IFM fractions. Protein concentrations from each fraction were determined and then either used immediately for functional analysis (Oxygraph, EPR, etc.) or treated with lysis buffer for Western blotting.

Mitochondrial Respiration. Mitochondrial respiratory function was studied according to published protocols (26). Oxygen consumption was measured using a Clark-type oxygen electrode (Oxygraph; Hansatech) during the sequential additions of substrates and inhibitors to purified mitochondria. Purified mitochondria (100–200 μg protein) were added to the oxymetry chamber in a 300-mL solution containing 100 mM KCl, 75 mM mannitol, 25 mM sucrose, 5 mM H3PO4, 0.05 mM EDTA, and 10 mM Tris·HCl, pH 7.2, at 37 °C. After 2 min of equilibration, 5 mM pyruvate and 5 mM malate were added, and oxygen consumption was followed for 1–2 min (state 4). ADP (250 μM) was added to measure state 3 (phosphorylating) respiration. To switch from NAD- to FAD-linked respiration, we first eliminated complex I through the inhibition of the back electron transfer using 0.5 mM rotenone and triggered complex II activity by the addition of 10 mM succinate. We inhibited complex III by the addition of 5 mM antimycin A. Complex IV activity was measured in the presence of 0.5 mM 2,2,4-trimethyl-1,3-pentanediol and 2 mM ascorbate. Oxygen use traces and rate determinations were obtained using Oxygraph software and normalized to protein.

Statistical Analysis. All data are presented as bar graphs and were analyzed using the GraphPad Prism 6 software (GraphPad Software, Inc.) as published previously (61). The data are depicted as mean ± SEM, and in all cases, $P < 0.05$ was considered statistically significant. For single comparisons, an unpaired t test was used. For Langendorff-perfused heart analysis as well as calcium swelling, we used a two-way ANOVA.

ACKNOWLEDGMENTS. We thank the Joan Heller Brown and Anne Murphy laboratories for providing us with neonatal cardiomyocytes and rat heart mitochondria. We appreciate the scientific input of Anna Busija and Yurong Gao. We thank Grace Liu for help in submitting the manuscript. The authors would like to thank the National Center for Microscopy and Imaging Research for providing the imaging resources. Funding for this research was provided by the AP Giannini Foundation (H.F.), Veterans Affairs Merit Award BX000783 (to D.M.R.), and National Institutes of Health Grants HL107200 (to D.M.R. and H.H.P.), HL091071 (to H.H.P.), DK54441 (to S.S.T.), and GM034921 (to S.S.T.).

1. Murry CE, Jennings RB, Reimer KA (1986) Preconditioning with ischemia: A delay of lethal cell injury in ischemic myocardium. *Circulation* 74(5):1124–1136.
2. Chiong M, et al. (2011) Cardiomyocyte death: Mechanisms and translational implications. *Cell Death Dis* 2:e244.
3. de Moissac D, Gurevich RM, Zheng H, Singal PK, Kirshenbaum LA (2000) Caspase activation and mitochondrial cytochrome C release during hypoxia-mediated apoptosis of adult ventricular myocytes. *J Mol Cell Cardiol* 32(1):53–63.
4. Mughal W, Dhingra R, Kirshenbaum LA (2012) Striking a balance: Autophagy, apoptosis, and necrosis in a normal and failing heart. *Curr Hypertens Rep* 14(6): 540–547.
5. Prech M, et al. (2010) Apoptosis as a mechanism for the elimination of cardiomyocytes after acute myocardial infarction. *Am J Cardiol* 105(9):1240–1245.
6. Edwards HV, Scott JD, Baillie GS (2012) The A-kinase-anchoring protein AKAP-Lbc facilitates cardioprotective PKA phosphorylation of Hsp20 on Ser(16). *Biochem J* 446 (3):437–443.
7. McKnight GS, et al. (1998) Cyclic AMP, PKA, and the physiological regulation of adiposity. *Recent Prog Horm Res* 53:139–159.
8. McConnachie G, Langeberg LK, Scott JD (2006) AKAP signaling complexes: Getting to the heart of the matter. *Trends Mol Med* 12(7):317–323.
9. Wehrens XH, et al. (2006) Ryanodine receptor/calcium release channel PKA phosphorylation: A critical mediator of heart failure progression. *Proc Natl Acad Sci USA* 103(3):511–518.
10. Hamdani N, et al. (2008) Myofilament dysfunction in cardiac disease from mice to men. *J Muscle Res Cell Motil* 29(6–8):189–201.
11. Zhang P, et al. (2012) Multiple reaction monitoring to identify site-specific troponin I phosphorylated residues in the failing human heart. *Circulation* 126(15):1828–1837.
12. Kitching R, et al. (2003) Characterization of a novel human breast cancer associated gene (BCA3) encoding an alternatively spliced proline-rich protein. *Biochim Biophys Acta* 1625(1):116–121.
13. Sastri M, Barraclough DM, Carmichael PT, Taylor SS (2005) A-kinase-interacting protein localizes protein kinase A in the nucleus. *Proc Natl Acad Sci USA* 102(2): 349–354.
14. León DA, Cànaves JM (2003) In silico study of breast cancer associated gene 3 using LION Target Engine and other tools. *Biotechniques* 35(6):1222–1231.
15. Gao F, Cheng J, Shi T, Yeh ET (2006) Neddylation of a breast cancer-associated protein recruits a class III histone deacetylase that represses NFkappaB-dependent transcription. *Nat Cell Biol* 8(10):1171–1177.
16. Gao N, Asamitsu K, Hibi Y, Ueno T, Okamoto T (2008) AKIP1 enhances NF-kappaB-dependent gene expression by promoting the nuclear retention and phosphorylation of p65. *J Biol Chem* 283(12):7834–7843.
17. Lu B, et al. (2012) Identification of hypertrophy- and heart failure-associated genes by combining in vitro and in vivo models. *Physiol Genomics* 44(8):443–454.
18. Tsutsui H, Kinugawa S, Matsushima S (2011) Oxidative stress and heart failure. *Am J Physiol Heart Circ Physiol* 301(6):H2181–H2190.
19. Giordano FJ (2005) Oxygen, oxidative stress, hypoxia, and heart failure. *J Clin Invest* 115(3):500–508.
20. King CC, Sastri M, Chang P, Pennypacker J, Taylor SS (2011) The rate of NF-κB nuclear translocation is regulated by PKA and A kinase interacting protein 1. *PLoS One* 6(4): e18713.
21. Zhang YL, Tavakoli H, Chachisvilis M (2010) Apparent PKA activity responds to intermittent hypoxia in bone cells: A redox pathway? *Am J Physiol Heart Circ Physiol* 299(1):H225–H235.
22. Baines CP (2010) The cardiac mitochondrion: Nexus of stress. *Annu Rev Physiol* 72: 61–80.
23. Ong SB, Gustafsson AB (2012) New roles for mitochondria in cell death in the reperfused myocardium. *Cardiovasc Res* 94(2):190–196.
24. Copeland DE, Dalton AJ (1959) An association between mitochondria and the endoplasmic reticulum in cells of the pseudobranch gland of a teleost. *J Biophys Biochem Cytol* 5(3):393–396.
25. Susin SA, et al. (1999) Molecular characterization of mitochondrial apoptosis-inducing factor. *Nature* 397(6718):441–446.
26. Clerk A, Sugden PH (2010) Dying by the way you live: AIF vs. caspases in apoptosis of hypertrophied cardiomyocytes. *Cardiovasc Res* 85(1):3–4.
27. Kurian GA, Berenshtein E, Saada A, Chevion M (2012) Rat cardiac mitochondrial sub-populations show distinct features of oxidative phosphorylation during ischemia, reperfusion and ischemic preconditioning. *Cell Physiol Biochem* 30(1):83–94.
28. Comelli M, Genero N, Mavelli I (2009) Caspase-independent apoptosis in Friend's erythroleukemia cells: Role of mitochondrial ATP synthesis impairment in relocation of apoptosis-inducing factor and endonuclease G. *J Bioenerg Biomembr* 41(1):49–59.
29. Marambio P, et al. (2010) Glucose deprivation causes oxidative stress and stimulates aggresome formation and autophagy in cultured cardiac myocytes. *Biochim Biophys Acta* 1802(6):509–518.
30. Ferreira RM, et al. (2012) Spatially distinct mitochondrial populations exhibit different mitofilin levels. *Cell Biochem Funct* 30(5):395–399.
31. Ali SS, Marcondes MC, Bajova H, Dugan LL, Conti B (2010) Metabolic depression and increased reactive oxygen species production by isolated mitochondria at moderately lower temperatures. *J Biol Chem* 285(42):32522–32528.
32. Marín-García J, Akhmedov AT, Moe GW (2012) Mitochondria in heart failure: The emerging role of mitochondrial dynamics. *Heart Fail Rev*, 10.1007/s10741-012-9330-2.
33. Nagasaka S, et al. (2007) Protein kinase A catalytic subunit alters cardiac mitochondrial redox state and membrane potential via the formation of reactive oxygen species. *Circ J* 71(3):429–436.
34. Sanz-Rosa D, García-Prieto J, Ibanez B (2012) The future: Therapy of myocardial protection. *Ann N Y Acad Sci* 1254:90–98.
35. Kuner R, et al. (2008) Genomic analysis reveals poor separation of human cardiomyopathies of ischemic and nonischemic etiologies. *Physiol Genomics* 34(1): 88–94.
36. Simkhovich BZ, Marjoram P, Poizat C, Kedes L, Kloner RA (2003) Brief episode of ischemia activates protective genetic program in rat heart: A gene chip study. *Cardiovasc Res* 59(2):450–459.
37. Meissner A, et al. (2000) The early response genes c-jun and HSP-70 are induced in regional cardiac stunning in conscious mammals. *J Thorac Cardiovasc Surg* 119(4 Pt 1): 820–825.
38. Marini M, et al. (2007) Mild exercise training, cardioprotection and stress genes profile. *Eur J Appl Physiol* 99(5):503–510.
39. Giusti B, et al. (2009) Gene expression profile of rat left ventricles reveals persisting changes following chronic mild exercise protocol: Implications for cardioprotection. *BMC Genomics* 10:342.
40. Gao N, Hibi Y, Cueno M, Asamitsu K, Okamoto T (2010) A-kinase-interacting protein 1 (AKIP1) acts as a molecular determinant of PKA in NF-kappaB signaling. *J Biol Chem* 285(36):28097–28104.
41. Boengler K, Heusch G, Schulz R (2011) Nuclear-encoded mitochondrial proteins and their role in cardioprotection. *Biochim Biophys Acta* 1813(7):1286–1294.
42. Chi NC, Karliner JS (2004) Molecular determinants of responses to myocardial ischemia/reperfusion injury: Focus on hypoxia-inducible and heat shock factors. *Cardiovasc Res* 61(3):437–447.
43. Leung TH, Ngan HY (2010) Interaction of TAp73 and breast cancer-associated gene 3 enhances the sensitivity of cervical cancer cells in response to irradiation-induced apoptosis. *Cancer Res* 70(16):6486–6496.
44. Hangen E, Blomgren K, Bénit P, Kroemer G, Modjtahedi N (2010) Life with or without AIF. *Trends Biochem Sci* 35(5):278–287.
45. Dawson VL, Dawson TM (2004) Deadly conversations: Nuclear-mitochondrial cross-talk. *J Bioenerg Biomembr* 36(4):287–294.
46. Cho BB, Toledo-Pereyra LH (2008) Caspase-independent programmed cell death following ischemic stroke. *J Invest Surg* 21(3):141–147.
47. Dispersyn GD, Borgers M (2001) Apoptosis in the heart: About programmed cell death and survival. *News Physiol Sci* 16:41–47.
48. Cribbs JT, Strack S (2007) Reversible phosphorylation of Drp1 by cyclic AMP-dependent protein kinase and calcineurin regulates mitochondrial fission and cell death. *EMBO Rep* 8(10):939–944.
49. Darshi M, et al. (2011) ChChd3, an inner mitochondrial membrane protein, is essential for maintaining crista integrity and mitochondrial function. *J Biol Chem* 286(4): 2918–2932.
50. Ginsberg MD, Feliciello A, Jones JK, Avvedimento EV, Gottesman ME (2003) PKA-dependent binding of mRNA to the mitochondrial AKAP121 protein. *J Mol Biol* 327(4):885–897.
51. Mukherjee SB, Das M, Sudhandiran G, Shaha C (2002) Increase in cytosolic Ca2+ levels through the activation of non-selective cation channels induced by oxidative stress causes mitochondrial depolarization leading to apoptosis-like death in Leishmania donovani promastigotes. *J Biol Chem* 277(27):24717–24727.
52. Boengler K, Schulz R, Heusch G (2009) Loss of cardioprotection with ageing. *Cardiovasc Res* 83(2):247–261.
53. Roth DM, et al. (2004) Indirect intracoronary delivery of adenovirus encoding adenylyl cyclase increases left ventricular contractile function in mice. *Am J Physiol Heart Circ Physiol* 287(1):H172–H177.
54. Reichelt ME, Willems L, Hack BA, Peart JN, Headrick JP (2009) Cardiac and coronary function in the Langendorff-perfused mouse heart model. *Exp Physiol* 94(1):54–70.
55. Tsutsumi YM, et al. (2006) Isoflurane produces sustained cardiac protection after ischemia-reperfusion injury in mice. *Anesthesiology* 104(3):495–502.
56. Patel HH, et al. (2006) Protection of adult rat cardiac myocytes from ischemic cell death: Role of caveolar microdomains and delta-opioid receptors. *Am J Physiol Heart Circ Physiol* 291(1):H344–H350.
57. Abramoff MD, Magalhaes PJ, Ram SJ (2004) Image processing with ImageJ. *Biophotonics International* 11(7):36–42.
58. Schindelin J, et al. (2012) Fiji: An open-source platform for biological-image analysis. *Nat Methods* 9(7):676–682.
59. Manders EM, Stap J, Brakenhoff GJ, van Driel R, Aten JA (1992) Dynamics of three-dimensional replication patterns during the S-phase, analysed by double labelling of DNA and confocal microscopy. *J Cell Sci* 103(Pt 3):857–862.
60. Palmer JW, Tandler B, Hoppel CL (1977) Biochemical properties of subsarcolemmal and interfibrillar mitochondria isolated from rat cardiac muscle. *J Biol Chem* 252(23): 8731–8739.
61. Fridolfsson HN, et al. (2012) Mitochondria-localized caveolin in adaptation to cellular stress and injury. *FASEB J* 26(11):4637–4649.